Journal of Molecular Liquids 225 (2017) 822–832

Contents lists available at ScienceDirect

Journal of Molecular Liquids

journal homepage: www.elsevier.com/locate/molliq

Enhanced prevention of progression of non alcoholic fatty liver to steatohepatitis by incorporating pumpkin seed oil in nanoemulsions

Sahar Youssef Al-Okbi [a], Doha Abdou Mohamed [a], Thanaa El-Sayed Hamed [a], Ahmed Alaa Kassem [b,*], Sameh Hosam Abd El-Alim [b], Dina Mahmoud Mostafa [b]

[a] Food Sciences and Nutrition Department, National Research Centre, Dokki, Cairo 12622, Egypt
[b] Pharmaceutical Technology Department, National Research Centre, Dokki, Cairo 12622, Egypt

ARTICLE INFO

Article history:
Received 12 September 2016
Received in revised form 29 October 2016
Accepted 31 October 2016
Available online 8 November 2016

Keywords:
Pumpkin seed oil
Oral nanoemulsions
Nutraceuticals
Food nanotechnology
Non-alcoholic steatohepatitis
Percolation phenomenon

ABSTRACT

Nanoemulsions (NEs) possess several advantages and have applications in controlled drug delivery and targeting. Pumpkin seed oil (PSO) oral NEs were dispensed with the objective of improving its oral bioavailability and prolonging its therapeutic efficacy. Phase diagrams were constructed. Eighteen formulations were selected from Labrafac™ PG phase diagrams. They passed thermodynamic stability tests and 10 out of them passed dispersibility tests in distilled water and 0.1 N HCl. Four formulations were compatible with PSO and showed total phenolic content ranging from 5.71 to 6.51 mg/kg of the incorporated PSO, expressed as gallic acid equivalent (GAE). The selected formulations revealed percolative electric conductivity, physiologically compatible pH, globule size <400 nm, optimum polydispersity index (PDI), negatively charged zeta potential values, and were sterically stabilized by Tween 80. The morphology investigation revealed spherical shaped globules using transmission electron microscopy. PSO NE formulation (F7), comprised of PSO (10%), Labrafac™ PG (17%), Tween 80 (31.5%), PEG 400 (31.5%) and water (10%) revealed the highest percent cumulative total phenolic content released after 24 h. F7 was evaluated for prevention of progression of fatty liver to steatohepatitis and fibrosis in a steatohepatitis and fibrosis induced rat model. Two oral doses (50 and 100 mg/kg rat body weight) were investigated thrice weekly. Results showed improvement of the different plasma lipid profile parameters as well as malondialdehyde and tumor necrosis factor-α, as representative of lipid peroxidation and inflammation, respectively, along with reduction of liver fat and improvement of hepatic function on treatment with PSO NE (F7); the high dose was more promising. Thus, incorporating PSO in nanosized NE system (F7) holds a promising technological approach to enhance the inhibition of the progression of fatty liver to steatohepatitis.

1. Introduction

Nutraceuticals are foods and food constituents that provide health benefits beyond basic nutrition. Evidence has suggested that dietary consumption of nutraceuticals is associated with decreased risks of multiple chronic diseases. However, many nutraceuticals have poor oral bioavailability [1]. An effective way to improve oral bioavailability of nutraceuticals is by encapsulating them in engineered nanoparticlulate based delivery systems [2,3].

The term nanoemulsions (NEs) refers to very fine dispersions possessing very small globule size which remain physically stable for long periods of time with no obvious sedimentation, flocculation or coalescence and reduce the possibility of creaming with Ostwald ripening. NEs have the property of drug targeting and controlled drug delivery. They possess several advantages as increased drug absorption leading to enhanced clinical potency accompanied with reduced therapeutic dose and consequently drug toxicity [4]. NE-based systems lead to higher bioavailability, more steady plasma drug levels and have been reported to prevail over intra and inter subject variations [5,6]. Therefore, NEs are considered as a promising tool to achieve controlled and targeted drug delivery because of their improved drug solubility, enhanced thermodynamic stability, extended shelf-life, rapid onset of action and decreased inter-subject variability [7]. NEs have potential advantages as nutraceutical and pharmaceutical delivery systems. Their small globule size and large surface area may lead to enhanced digestion rates, faster formation of mixed micelles, higher release of bioactive agents, more rapid diffusion across the mucus layer and improved epithelium cell permeability [8]. Moreover, they may inhibit the oxidation of chemically labile bioactive compounds, thereby increasing their shelf-life and reducing their degradation in the

* Corresponding author at: Pharmaceutical Technology Department, National Research Centre, El-Buhouth Street, Dokki, Cairo 12622, Egypt.
E-mail address: aa.kassem@hotmail.com (A.A. Kassem).

http://dx.doi.org/10.1016/j.molliq.2016.10.138
0167-7322/

gastrointestinal tract (GIT) [9]. Recently, increased attention has been focused on the utilization of NEs to encapsulate and deliver bioactive agents, as nutraceuticals [10,11].

Non-alcoholic fatty liver disease (NAFLD) is a commonly occurring disorder among the Egyptian population, and is considered as the hepatic constituent of metabolic syndrome and it is more prevalent among obese and diabetic humans. NAFLD is the most frequent cause of chronic liver injury globally. Deposition of liver fat (steatosis) *per se* does not represent a health risk. However incidence of high oxidative stress and inflammation due to excessive accumulation of liver fat could lead to development of non-alcoholic steatohepatitis (NASH) (fatty liver with inflammation) [12] which is a major risk factor for development of cardiovascular disease (CVD) on one hand [13,14]. On the other hand, if steatohepatitis is not managed it could progress to liver fibrosis, cirrhosis, hepatocarcinoma and liver failure in the end stage [15–18]. No exact drug therapies are used for fatty liver diseases, however, ursodeoxycholic acid, insulin sensitizer and blood lipid lowering drugs can somehow improve the condition [19–21].

Recently, researchers have paid attention to scientific investigation of dietary plants and herbal preparations as alternative clinical therapies [22]. Pumpkin plant has been commonly used as food or medicine [22]. The pumpkin (genus *Cucurbita*) belongs to the family *Cucurbitaceae* [22,23]. *Cucurbita pepo* L., *Cucurbita maxima* Duchesne, and *Cucurbita moschata* Duchesne are cultivated extensively worldwide as they are considered economically important species [22]. Pumpkins have been grown for production of oil in Austria, Hungary and Slovenia for the last three hundred years [24]. It is declared that *C. pepo* produces the highest quality oil due its higher persistency and lower liability to deterioration [25]. Pumpkin seed oil (PSO) is a rich natural source of triterpenes, phytosterols, antioxidative phenolic compounds, polyunsaturated fatty acids, tocopherol and carotenoids [23]. PSO was reported to have therapeutic potential towards hypertension, atherosclerosis, prostatic hypertrophy, urinary bladder hyperplasia and tapeworm [26–29]. Consumption of high quantity of PSO has shown to improve fatty liver and oxidative injury in rats fed high fructose diet [30].

The objective of this study is the fabrication of PSO in NE delivery systems to increase the oral bioavailability and to test the acquired enhanced therapeutic potential in a progressive rat model of steatohepatitis through feeding high fructose diet deficient in methionine and choline chloride.

2. Materials and methods

2.1. Materials

Pumpkin seed oil (PSO) 100% Virgin (*Cucurbita pepo*, L. Family *Cucurbitaceae*) was obtained from Ölmühle Pelzmann GmbH, Graz, Austria. PSO used in the present study contains tocopherols (275.08 mg/100 g), phytosterols (43% of total unsaponifiable fraction), as well as linoleic and oleic acids (38.9 and 3.5% of total fatty acids, respectively), as reported in a previous study [31]. It has an *in vitro* antioxidant activity of 85.5% as previously determined by ferric thiocyanate method [32]. Labrafac™ PG (propylene glycol dicaprylocaprate EP, propylene glycol dicaprylate/dicaprate NF) and Maisine™ 35–1 (glycerol monolinoleate EP, glycerol monolinoleate NF) were kindly donated by Gattefosse, Saint-Priest Cedex, France. Tween 80 (polysorbate 80), polyethylene glycol (PEG) 400 and Folin-Ciocalteu reagent (FCR) were purchased from Sigma Aldrich Co., St Louis, Mo, USA. All other chemicals were of analytical grade.

2.2. Methods

2.2.1. Construction of pseudo-ternary phase diagrams

Prior to the construction of the phase diagrams to elucidate the NE existence zones, a miscibility study for PSO (tested active oil) with Labrafac™ PG and Maisine™ 35–1 (carrier oils) was conducted. Both oils were employed, each with Tween 80 (surfactant) and PEG 400 (co-surfactant) in surfactant/co-surfactant (Smix) ratios 1:1, 2:1 and 3:1. The oil/Smix weight ratios ranged from 1:9 to 9:1. Oil and Smix were mixed gently, and then water was added dropwise, followed by stirring on a vortex mixer and left to equilibrate for 24 h. The systems were checked for homogeneity and clarity visually [33–36]. The formation of the NE was considered as clear/transparent and easily dispersible NE and marked on the pseudo-ternary phase diagram. Phase diagrams were constructed to reveal the NE existence zones. The phase diagram was plotted using SigmaPlot (version 11.0) ternary plot software.

2.2.2. Selection of NE systems from phase diagrams

Eighteen NE systems were selected from the pseudo-ternary phase diagrams employing Labrafac™ PG as the oil phase. The systems with 63, 60 and 57% Smix are presented in Table 1.

2.2.3. Thermodynamic stability study

The test was performed for the 18 NE systems by centrifugation at 5000 rpm for 30 min [37] and checked for phase separation, creaming or cracking.

2.2.4. Dispersibility studies

The dispersibilty studies were conducted to evaluate the efficiency of dispersibility of oral NEs. One mL of each of the 18 systems were added to 500 mL distilled water and 0.1 N HCl in a dissolution rate tester (Dissolution Test Station, Hanson SR8 Plus, New Jersey, USA) apparatus II with paddle speed 50 rpm at 37 ± 0.5 °C. The systems were evaluated using the grading scale reported by Bali et al. [38].

Grade A: refers to rapidly forming (within 1 min) NE, having a clear or bluish appearance.

Grade B: is rapidly forming (within 2 min), slightly less clear NE, having a bluish white appearance.

Grade C: is fine milky emulsion that was formed within 2 min.

Grade D: is dull, grayish white emulsion having slightly oil appearance that is slow to emulsify (longer than 2 min).

Grade E: is a formulation, exhibiting either poor or minimal emulsification with large oil globules present on the surface (longer than 3 min).

Formulations those passed this test in grade A or B were selected for further optimization.

2.2.5. Preparation of PSO NEs

The NE systems passing the dispersibility test were used to dispense PSO NEs. PSO was incorporated as 10% of the NE system, its composition subtracted from the carrier oil phase; Labrafac™ PG. The oils were mixed and Smix added. The mixture was mixed on a vortex mixer again, and then sonicated using (Branson 2510E–DHT, Richmond, VA, USA) bath sonicator for 15 min. The systems revealing incompatibility with PSO; by showing phase separation after equilibration, were excluded from further investigations.

2.2.6. Evaluation of total phenolic content in PSO incorporated in NEs

The amount of total phenolic content, expressed as gallic acid equivalent (GAE) mg/kg, was determined in PSO incorporated in NEs. Prior to evaluation, calibration curve for gallic acid in methanol was constructed. For assaying the total phenolic content in PSO NEs, 0.1 mL of NE was diluted 50-folds using methanol, followed by bath sonication for 1 h. Afterwards, 0.5 mL of the sonicated mixture was taken to which 2.5 mL dilute FCR in distilled water (1:9 v/v) and 2 mL sodium carbonate (7.5% w/v) solution were added [39]. The reaction mixture was vortexed and incubated in the dark for 24 h, then assayed spectrophotometrically at 745 nm for encapsulated total phenolic content [36]. The evaluation was conducted in triplicate.

Table 1
Composition, thermodynamic stability and dispersibility study of selected NE formulations.

Formulation	Oil (%) Labrafac™ PG	Surfactant (%) Tween 80	Co-surfactant (%) PEG 400	Smix Ratio	Smix %	Water %	Oil/Smix Ratio	Thermodynamic stability Centrifugation study	Dispersibility Distilled water	Dispersibility 0.1 N HCl	Inference
F1	15.75	31.5	31.5	1:1	63	21.25	2:8	Passed	Grade A	Grade A	Passed
F2	15.75	42	21	2:1	63	21.25	2:8	Passed	Grade B	Grade C	Failed
F3	15.75	47.25	15.75	3:1	63	21.25	2:8	Passed	Grade B	Grade C	Failed
F4	15	30	30	1:1	60	25	2:8	Passed	Grade A	Grade A	Passed
F5	15	40	20	2:1	60	25	2:8	Passed	Grade B	Grade C	Failed
F6	15	45	15	3:1	60	25	2:8	Passed	Grade B	Grade C	Failed
F7	27	31.5	31.5	1:1	63	10	3:7	Passed	Grade A	Grade A	Passed
F8	27	42	21	2:1	63	10	3:7	Passed	Grade A	Grade A	Passed
F9	27	47.25	15.75	3:1	63	10	3:7	Passed	Grade B	Grade C	Failed
F10	25.72	30	30	1:1	60	14.28	3:7	Passed	Grade A	Grade A	Passed
F11	25.72	40	20	2:1	60	14.28	3:7	Passed	Grade A	Grade A	Passed
F12	25.72	45	15	3:1	60	14.28	3:7	Passed	Grade B	Grade C	Failed
F13	14.25	28.5	28.5	1:1	57	28.75	2:8	Passed	Grade A	Grade A	Passed
F14	14.25	38	19	2:1	57	28.75	2:8	Passed	Grade A	Grade A	Passed
F15	14.25	42.75	14.25	3:1	57	28.75	2:8	Passed	Grade A	Grade A	Passed
F16	24.43	28.5	28.5	1:1	57	18.57	3:7	Passed	Grade C	Grade C	Failed
F17	24.43	38	19	2:1	57	18.57	3:7	Passed	Grade A	Grade A	Passed
F18	24.43	42.75	14.25	3:1	57	18.57	3:7	Passed	Grade C	Grade C	Failed

2.2.7. Characterization of selected NEs

Based on dispersibility study and PSO incorporation compatibility results, four NE systems were selected to perform characterization and further investigations. NEs were characterized for their morphology, pH, electric conductivity, globule size and zeta potential.

2.2.7.1. Transmission electron microscopy (TEM). Selected NEs were photographed using TEM, JEOL JEM-2100 (JEOL Co., Tokyo, Japan), under a high tension electricity of 160 kV. Samples were diluted (1:100) using double distilled water [40]. One drop was placed on a carbon-coated grid, stained with 1% phosphotungstic acid (w/v) and left to dry on a filter paper for 2 min. The samples were then loaded to the microscope and examined at appropriate magnifications.

2.2.7.2. Electric conductivity and pH measurements. The electric conductivity (σ) and pH of the selected formulations were examined at room temperature using the conductivity/pH meter, Thermo Scientific Orion VERSA STAR™ Advanced Electrochemistry Meter, VSTAR 92 (Thermo Fisher Scientific Inc., USA). Conductivity measurements were carried out by titration of oil-Smix with double distilled water. The systems investigated were Labrafac™ PG/Smix (3:7) at Smix ratios of Tween 80/PEG 400 (1:1) (System A) and (2:1) (System B) diluted dropwise with double distilled water. Measurements were considered after reaching equilibrium. The data was expressed in terms of weight fraction Φ_w (% wt) of aqueous component [41] which is defined as Eq. (1):

$$\Phi_w(\%\mathrm{wt}) = \frac{\text{wt. of double distilled water}}{\text{total wt. of nanoemulsion}} \times 100 \quad (1)$$

2.2.7.3. Globule size analysis. The globule size of the selected NEs and its distribution, characterized by polydispersity index (PDI), were measured for (1:100) diluted samples with double distilled water [40,42] at 25 °C by dynamic light scattering (DLS) using Particle and Zetasizer Nano-ZS (Malvern Instruments, Worcestershire, UK).

2.2.7.4. Zeta potential measurements. Further, the selected formulations were evaluated for zeta-potential by dynamic light scattering (DLS) employing Particle and Zeta-sizer Nano-ZS (Malvern Instruments, Worcestershire, UK) after (1:100) dilution using double distilled water [37].

2.2.8. In vitro drug release study

The *in vitro* release study was performed for 1 mL of each selected formulation, using dialysis bags (Dialysis tubing cellulose membrane, Sigma Co., USA; Molecular weight cutoff 12,000–14,000) in 50 mL distilled water; dissolution medium [37], at 37 ± 0.5 °C using the isothermal shaker (GFL 3032, Germany). The speed was adjusted to 75 rpm and aliquot samples were withdrawn at 1, 2, 3, 4, 6, 8 and 24 h and replaced with fresh medium. The samples were filtered through 0.45 μm pore-sized nylon syringe filter and analyzed spectrophotometrically at 745 nm for released total phenolic content [39], as previously discussed. Further, percent cumulative total phenolic content released was calculated and plotted *versus* time in the release profile. Each formulation was assessed in triplicate.

2.2.9. In vivo evaluation

2.2.9.1. Animals. Male Sprague Dawley rats weighing 100–140 g were used in the present study. Animals were obtained from the animal house of the National Research Centre, Cairo, Egypt. Animals were kept individually in stainless steel cages; water and food were given *ad-libtium* and exposed to alternating 12 h of light and darkness. The care of the rats as well as the conducted animal experiments were in accordance with the institutional ethical guidelines, and were approved prior by the Institutional Animal Ethics Committee (Medical Research Ethics Committee (MREC) of the National Research Centre, Cairo, Egypt).

2.2.9.2. Diets. Experimental diets were prepared as illustrated in Table 2. Salt mixtures and vitamin mixtures were prepared according to Briggs and Williams [43] and Morcos [44], respectively. Another vitamin mixture was prepared free from choline chloride. Oil soluble vitamins were given orally in a dose of 0.1 mL/rat per week. Methionine and choline

Table 2
Composition of different diets (g per 100 g).

Ingredients	Methionine and choline deficient-high fructose diet	Balanced diet
Casein	17	12
Corn oil	–	10
Butter fat	5.5	–
Fructose	70	–
Starch	–	70.2
Salt mix.	3.5	3.5
Vitamin mixture (free from choline chloride).	1	–
Vitamin mixture (including choline chloride)	–	1
Methionine	–	0.3
Cellulose	3	3

deficient-high fructose diet (MCFD) was prepared according to Kawasaki et al. [45] and Deminice et al. [46] to induce steatohepatitis in rats.

2.2.9.3. Experimental design. Twenty-four rats were divided into four groups, each of six rats. The first group was considered as the normal healthy group where rats received a balanced diet. The second group was fatty liver control where rats were fed on MCFD. Rats of group three and four were fed on MCFD and given oral dose of the selected PSO NE formulation (50 and 100 mg/kg rat body weight, respectively) thrice a week. During the experiment, body weight and food intake were recorded weekly. After thirty-five days (end of the study) total food intake, body weight gain and food efficiency ratio (body weight gain/total food intake) were calculated. Blood samples were collected from all rats after an overnight fast for the determination of plasma total cholesterol (T-Ch) [47], high density lipoprotein cholesterol (HDL—Ch) [48], low density lipoprotein cholesterol (LDL-Ch) [49] and triglycerides (TG) [50] by colorimetric methods. HDL-Ch/T-Ch ratio was calculated as indicator of cardiovascular diseases risks. Malondialdehyde (MDA) was determined as representative of lipid peroxidation [51] by colorimetric method. Plasma tumor necrosis factor-α (TNF-α) (an inflammatory biomarker) [52] was assessed by enzyme-linked immunosorbent assay. The activity of aspartate transaminase (AST) and alanine transaminase (ALT) [53], plasma albumin [54], total and direct bilirubin [55], and alkaline phosphatase (ALP) [56] were estimated by colorimetric methods as indicators of liver function. Liver was immediately removed, weighed and stored at −20 °C till analyzed. Hepatic lipids were extracted and weighed according to the procedure of Folch et al. [57] and Cequier-Sànchez et al. [58] and the concentration of triglycerides [50] and cholesterol [47] was measured colorimetrically using commercial kits.

2.2.10. Statistical analysis

The results were expressed as the mean ± SE and analyzed statistically using one-way analysis of variance (ANOVA) followed by Duncan's post-hoc test. In all cases, $P < 0.05$ was used as the criterion of statistical significance.

3. Results and discussion

3.1. Pseudo-ternary phase diagrams and formulations selection

Prior to construction of phase diagrams, the miscibility study of PSO (tested active oil) with Labrafac™ PG and Maisine™ 35–1 (carrier oils) showed complete miscibility and hence, both carrier oils were considered to construct the phase diagrams, each with Tween80/PEG400 (Smix) and double distilled water. Three phase diagrams, illustrating 3 Smix ratios; 1:1, 2:1 and 3:1, were plotted for each oil. The phase diagrams are demonstrated in Fig. 1. Phase diagrams are utilized to learn the phase behavior of NE systems. Formation of NEs is vitally dependant on the successful selection of oil, surfactant, co-surfactant and their mixing ratios [59]. Non-ionic or zwitterionic surfactants are commonly used for NE formulation due to their reduced toxicity and resistance to pH and ionic strength alterations [60]. In the present study, Tween 80; non-ionic surfactant was employed. The phase diagrams (Fig. 1) elucidate the large NE existence zone on employing the oil; Labrafac™ PG compared to the smaller zone exhibited on employing Maisine™ 35–1. These results propelled the authors to proceed with the work using Labrafac™ PG as the oil phase. The degree by which surfactant decreases the interfacial tension of the oil–water interface and changes in dispersion entropy, influences the free energy of NE formation [61,62], and the present results demonstrated that increasing surfactant proportion (Smix 1:1, 2:1 and 3:1) led to a larger NE existence zone (Fig. 1). The surfactant lowers the interfacial tension of the oil–water interface by arranging the polar heads towards the aqueous phase and non-polar tail pull out oil phase, thus forming a stabilizing layer around the oil globule [62,63]. Therefore, the approached NE for oral drug delivery is the NE system in which the amount of surfactant or the Smix is able to reduce the interfacial tension, enhance the dispersion entropy, lower the system free energy to a extremely small value and augment the interfacial area [37]. Hence, from the phase diagrams of Labrafac™ PG, 18 systems (Table 1) were selected to proceed with, employing 3 Smix percentage compositions; 63, 60 and 57%.

3.2. Thermodynamic stability study

It is reported that conventional emulsions are kinetically unstable and will ultimately phase separate, on the other hand NEs are thermodynamically stable [64]. The 18 NEs, chosen from the pseudo-ternary phase diagrams employing Labrafac™ PG as the carrier oil, passed the thermodynamic stability study by centrifugation at 5000 rpm for 30 min (Table 1). No phase separation was observed and proceeding with the dispersibilty studies was performed for the 18 NE systems.

3.3. Dispersibilty studies

The main purpose of the dispersibilty test is to evaluate the stability of NE upon dispersion in GIT fluids. Due to dilution, there may exist phase separation, eventually leading to precipitation of the drug [62]. After oral administration, the GIT fluids will dilute the NE and consequently the surfactant layer, surrounding the oil globule, will be gradually desorbed. The process is thermodynamically governed by the need of the surfactant to keep an aqueous phase concentration equal to its critical micelle concentration [62]. Ten formulations passed the dispersibilty studies (Table 1), in both media, with grade A and were selected to continue for further investigations.

3.4. Preparation of PSO NEs

The NE systems passing the dispersibility tests were considered for PSO incorporation. PSO was incorporated as 10% of the NE systems, subtracted from carrier oil phase of the formulations. F1, F4, F13, F14, F15 and F17 showed PSO incompatibility with the NE systems resulting in phase separation, after equilibrium. It seems that the nature of PSO does not allow easy dispersion and emulsification in the NE systems on using the Smix type and amount employed in the formulations prepared. Hence, when the carrier oil, which formerly showed complete compatibility and perfect formation of NE systems, is low, as encountered in the aforementioned formulations, excluding F17, the higher oil ratio favors PSO and not the carrier; Labrafac™ PG leading to phase separation. However, F17 holds high oil content, so the phase separation may be explained by the low Smix composition; 57%, which seems to be insufficient for emulsification of PSO in the NE system. It is noteworthy that the surfactant used; Tween 80, is a non-ionic surfactant which is reported to resist pH changes and effects of electrolytes in addition to its lower irritancy [65]. The co-surfactant used; PEG 400 aids the surfactant in further reducing the surface tension of the system [65]. It is reported that PEG 400 is a non-toxic, water soluble and neutral polymer used by the FDA for internal consumption and injection, and introduced into several biomaterials and drugs because of non-immunogenicity [66]. It is also reported that the NE formation is non-spontaneous because the total free energy required is positive. This depends on the surfactant capacity to lower the interfacial tension at oil/water interface thus decreasing the free energy required [67]. It has been established that the surfactant concentration should be minimum as possible, therefore its concentration ought to be carefully calculated [38]. From the mentioned discussion, it is important to use the least surfactant concentration to obtain a homogenous stable NE system. The formulations showing compatibility with PSO; F7, F8, F10 and F11 hold optimum surfactant concentrations ranging from 30 to 42% in the Smix compositions employed. The high oil content; 25–27%, in these systems, ensures the formation of homogenous compatible PSO NEs.

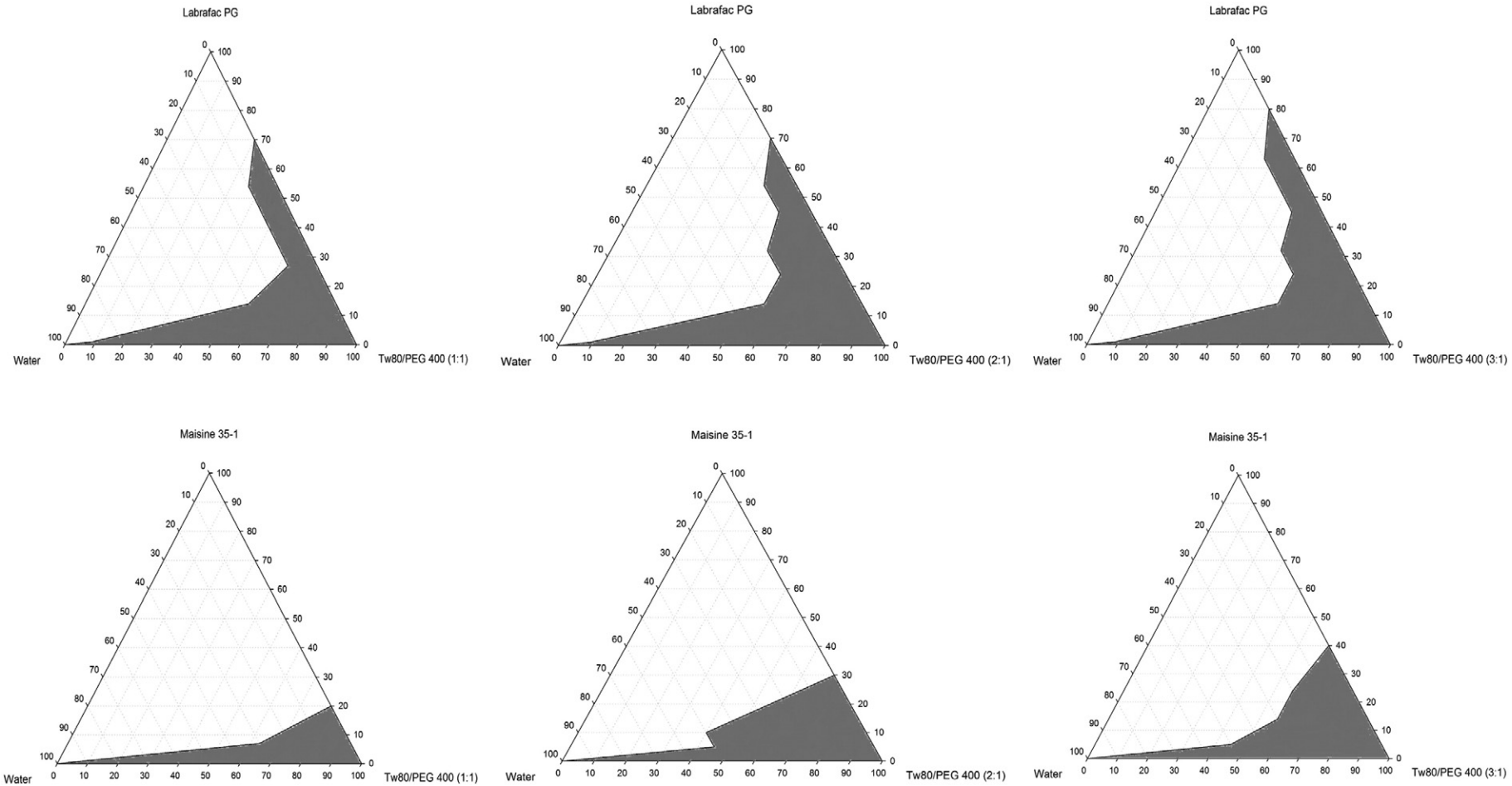

Fig. 1. Pseudoternary phase diagrams employing Labrafac™ or Maisine™ 35–1 as oil phase, Tween 80 as surfactant and PEG 400 as co-surfactant. Shaded areas represent the transparent o/w nanoemulsion existence zone.

3.5. Evaluation of total phenolic content in PSO incorporated in NEs

The results of total phenolic content, expressed as percent gallic acid equivalent (GAE) mg/kg, in PSO incorporated in the 4 selected NE systems, are presented in Table 3. The total phenolic content ranged from 5.71 to 6.51 mg/kg which is in accordance to a previous report [68] where the total phenolic content was found to be 4.63 ± 0.45 mg/kg in cold-pressed PSO, whereas higher content of total phenolic compounds was reported in oil samples obtained from roasted seeds; from 13.46 ± 0.27 to 19.60 ± 1.23 mg/kg [68]. Furthermore, higher contents of phenolics, in a range from 24.71 to 50.93 mg/kg as GAE, were found by Andjelkovic et al. [69]. These results further confirm the non-roasted nature [70] of the virgin PSO employed in the present study, with no higher estimation of phenolic contents in the oil due to thermal treatment as reported for roasted seeds [68].

The total phenolic content assay by FCR is simple, convenient and reproducible. It is a commonly accepted assay and routinely practiced in dietary antioxidant research laboratories all over the world. As a result, a large body of data has been accumulated, and it has become a routine assay in studying phenolic antioxidants [71]. However, it has some limitations and disadvantages, especially when the raw material has been roasted [72]. According to Huang et al. [71], the FCR assay measures sample reducing capacity, which does not reflect the total phenolic content. The Maillard reaction products, formed during roasting give a positive result with the FCR, and their impact cannot be neglected when the FCR is used. Nevertheless, a large body of comparable data has been produced *via* the FCR assay and claimed as total phenolic content instead of reducing capacity of FCR [71].

3.6. Characterization of selected NEs

3.6.1. Transmission electron microscopy (TEM)

The investigation of microstructures' morphology as NEs using TEM, is one of the most important techniques because it directly photographs high resolution images and can capture any concurrent structures and microstructure transitions [6]. TEM of the selected NE systems are exhibited in Fig. 2. The NE globules appeared as spherical bright globules and the surroundings were dark. The globules emerged clearly with no signs of aggregation or coalescence.

3.6.2. Electric conductivity and pH measurements

Table 3 show the pH measurement results of the four selected NE formulations. Increasing the water content from 10 to 14.28% showed a slight decrease in the pH values. Incorporation of the PSO caused no significant change in the pH values as well. Nevertheless, the observed pH values are considered physiologically acceptable [73]. Electric conductivity (σ) was measured as a function of water content Φ_w (wt%) for the oil-Smix [41,74] (Fig. 3). Fig. 3 reveals the results of variation of σ *versus* water content Φ_w (wt%). The pattern shows profile characteristic of percolative conductivity [75,76], where the electric conductivity is initially low but increases with increase in aqueous phase. The electric conductivities of the two selected systems remained roughly zero at Φ_w values below 10% (w/w) (Fig. 3). During the dropwise addition of water up to $\Phi_w \approx 65\%$ (w/w), a fast increase of σ was observed. At $\Phi_w > 65\%$ (w/w), the conductivities of both systems were not significantly affected by the further additions of water. The low conductivity values below Φ_p suggests that the reverse droplets are discrete (isolated droplets in a non-conducting Labrafac PG medium, forming w/o NE) and have little interaction. While the water quantity increases, the electric conductivities of the investigated systems slightly increases concurrently until the critical Φ_w is reached where a sudden increase in conductivities is observed. This phenomenon is known as percolation, and the critical Φ_w at which it is occurs is known as percolation threshold (Φ_p) [77,78]. Away from the percolation threshold ($\Phi_p \approx 10\%$ (w/w) conductivity increases linearly and steeply up to $\Phi_w \approx 65\%$ (w/w). Accordingly, it might be concluded that away from Φ_p a network of conductive channels exists, which corresponds to the formation of water cylinders or channels in an oil phase due to the attractive interactions between the spherical nanodroplets of water phase in the w/o NE (bicontinuous NE) [41,74,78]. For the $\Phi_w > 65\%$ (w/w) the electric conductivities increase non-linearly up to $\Phi_w \approx 75\%$ (w/w). This non-linear increase of the conductivity can be attributed to further modifications in the medium where a continuous growing and interconnecting of the aqueous microdomains takes place [79]. After reaching $\Phi_w \approx 75\%$ (w/w), further additions of water, slightly decreased the electric conductivities of both systems, and these findings might be explained by the dilution of o/w NE with the added water which decreased the concentration of the dispersed oil droplets [80,81]. Hence, the σ–Φ_w curve illustrates the incidence of the three structural regions: w/o [$\Phi_w < 10\%$ (w/w)], nonspherical w/o–bicontinuous–non-spherical o/w [10% (w/w) $< \Phi_w < 65\%$ (w/w)], and o/w [$\Phi_w > 65\%$ (w/w)] [78].

3.6.3. Globule size analysis

NE behavior is clearly understood by investigating its globule size. Furthermore, the globule size influence the composition and the bio-acceptability of the delivery system [38]. The globule size of the prepared NEs is expressed in Table 3. It is clear that F7 possessed the smallest globule size which increased sequentially up to F11. F7 and F8 acquired lower NE globule size because of higher content of Smix; 63% compared to F10 and F11 with 60% Smix content. Tween 80; the non-ionic surfactant employed in this study (HLB = 15) is more effective in decreasing globule size in contrast to PEG 400 because of its rapid adsorption onto droplet surface [82]. The reduction in NE globule size with increasing surfactant concentration as encountered in the study, is in agreement with a previous report [83]. All formulations showed PDI values <0.5, indicating uniform globule size distribution [84].

3.6.4. Zeta-potential measurements

The surface charge of the emulsion globules is generally characterized by zeta potential. Physical stability of the multiphase systems may be improved by repulsive forces between globules acquired by high absolute zeta potential values [85]. The values of zeta potential of selected NEs are illustrated in Table 3. The moderately low values of zeta potential possessed by the NEs might be due to the presence of relatively increased concentrations of Tween 80, employed in the formulations. Electrostatic and steric repulsion are the two main stabilizing forces for NEs [86]. It is reported that the relatively large hydrophilic (polyoxyethylene) head groups of adsorbed Tween molecules on the surface of NE oil droplets results in steric stabilization against

Table 3
Total phenolic content, pH, electric conductivity, globule size, polydispersity index and zeta potential of selected NE formulations.

Formulation	System	Φ_w (wt%)	Total phenolic content expressed as (GAE) mg/kg ± S.E.	pH		σ (μS/cm)		Globule size (nm) ± S.E.	PDI*	Zeta potential (mV) ± S.E.
				Unloaded	Loaded	Unloaded	Loaded			
F7	A	10	6.51 ± 0.39	4.94	4.84	3.12	4.56	198.90 ± 42.03	0.366	-9.10 ± 2.16
F8	B	10	6.15 ± 0.27	5.20	5.09	6.24	8.77	217.30 ± 38.39	0.306	-7.66 ± 2.65
F10	A	14.28	5.75 ± 0.06	4.79	4.66	10.40	14.17	313.40 ± 79.79	0.441	-7.70 ± 2.01
F11	B	14.28	5.71 ± 0.70	4.96	4.87	12.37	15.53	356.20 ± 93.57	0.455	-5.01 ± 2.39

* PDI = Polydispersity index.

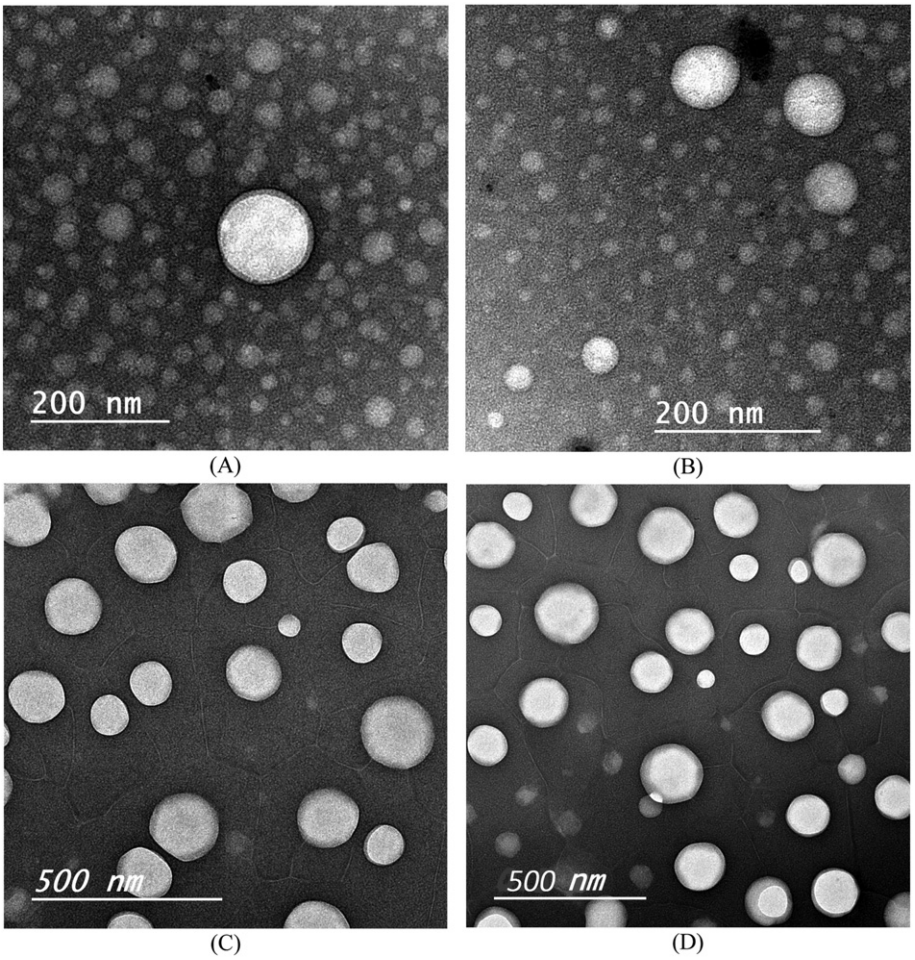

Fig. 2. Transmission electron microscope micrographs of selected PSO NE formulations: (A) F7, (B) F8, (C) F10 and (D) F11.

aggregation by steric (rather than electrostatic) repulsion [87]. These reports go in agreement with the findings of this research.

3.7. In vitro drug release study

Release study by dialysis bags is conducted to compare the release profiles of total phenolic content from the four selected PSO NEs. The highest release is encountered by F7 followed by F8 then F10 and finally F11 (Fig. 4). The percent cumulative total phenolic content released after 24 h reached 100% for F7, 78.32% for F8, 74.41% for F10 and the least value; 60.48% for F11. The reason behind the high release from F7 is the small globule size which offers a large surface area for the release of the encapsulated phenolic compounds therefore facilitating

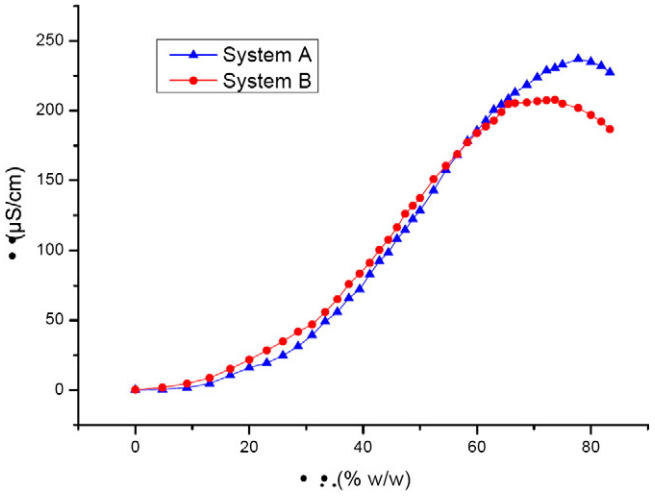

Fig. 3. Electrical conductivity (σ) as a function of water phase volume fraction (Φ_w). Labrafac™ PG/Smix (3:7) at Smix ratios of Tween 80/PEG 400 (1:1) (System A) and (2:1) (System B).

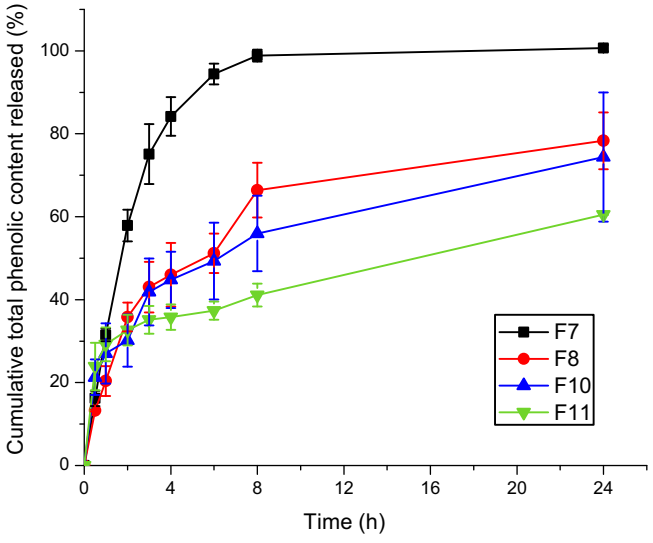

Fig. 4. Comparative *in vitro* release profiles of total phenolic content from selected PSO NE formulations. Data presented as mean ± S.E.

higher phenolic dissolution. These findings are in agreement with previous reports [37,40,88].

Accordingly, formulation F7 showing optimum total phenolic content, small globule size and highest cumulative percent total phenolic content released after 24 h, is the optimized formulation and is selected for carrying out the pharmacodynamic *in vivo* evaluation.

3.8. In vivo evaluation

Table 4 show different biochemical parameters of control normal and fatty liver rats. Plasma levels of total and direct bilirubin and plasma activities of AST, ALT and ALP were increased significantly with significant reduction of albumin in rats fed MCFD (control fatty liver), indicating liver dysfunction. Treatment with PSO NE with feeding MCFD resulted in significant reduction in AST, ALT and ALP activity and total and direct bilirubin with elevation of albumin compared with control fatty liver rats. Control fatty liver rats exhibited a significant increase in plasma total cholesterol, triglycerides, LDL-Ch and the ratio of T-Ch/HDL-Ch compared with the control normal rats. In addition; significant increases were observed in total fat, T-Ch and TG in the liver tissue of MCFD-fed rats compared to control normal. Rats treated with PSO NEs revealed significant improvement in plasma lipid profile and reduction in the contents of liver total fat, T-Ch and TG with different degrees. Plasma levels of MDA increased significantly in MCFD-fed rats compared with normal control. Rats fed on MCFD and treated with PSO NE showed significant reduction in MDA levels but still higher than normal rats. Plasma level of TNF-α was significantly higher in MCFD group than normal rats group. This elevation was reduced significantly in rats fed on MCFD and treated with PSO NEs. The improvement of the different biochemical parameters on administration of PSO NEs was dose dependent where the high dose (100 mg/kg) showed significant improvement compared with the low dose (50 mg/kg). Plasma HDL-Ch, T-Ch/HDL-Ch and direct bilirubin were normalized on treatment with the high dose (100 mg/kg).

Nutritional parameters and liver weight/body weight % of normal and fatty liver rats are shown in Table 5. The results revealed non-significant changes ($P > 0.05$) of the aforementioned parameters among all groups.

In the present study, MCFD was used to induce a model of NAFLD in rats. Feeding MCFD induced dyslipidemia, liver dysfunction, elevated oxidative stress represented by MDA and inflammation reflected in the elevated TNF-α as well as increased hepatic fat which verify the induction of NASH. The significant increase in T-Ch/HDL-Ch also showed high risk to CVD.

Choline is an essential substance that is implicated in many metabolic reactions in rats (such as methylation or transport of lipids). It is employed for the formation of many biologically important compounds, such as sphingomyelin, phosphatidylcholine (PC) and acetylcholine. PC is crucial for the normal VLDL formation and its secretion from the liver. In case of choline absence in the diet, methionine substitute it for the synthesis progression. Both choline and methionine are considered as lipotropic agents and their deficiency will lead to a significant disturbance in the formation of PC [89]. Feeding rats a methionine-choline deficient diet (MCDD) promotes triglycerides to accumulate rapidly in the liver with the consequent development of steatohepatitis and fibrogenesis [90]. In contrast to MCDD, sufficient addition of methionine to a choline-deficient diet does not cause blockage of VLDL secretion, thus leading to steatosis with a lesser degree of inflammation in the rat liver [90,91]. The manifestations of losing weight and proportional decrease of the liver weight as a result of malnutrition, are observed in rats fed with MCDD [90] which is not the case in the present study because the diet in addition contains high fructose. MCDD induces liver injury with simultaneous elevation of serum transaminases and pro-inflammatory cytokines, such as IL-1β, IL-6 and TNF-α [92] which agreed with the present results. This model is more appropriate for studying the consequences of fat accumulation, inflammation, oxidative stress and fibrogenesis in the liver than the complex pathogenesis of human NAFLD. The presence of high fructose in the present diet has a synergistic effect in induction of NASH.

In humans, consumption of high quantities of fructose in the diet is accompanied by metabolic syndrome, obesity and NAFLD [93]. High fructose potentiates protein fructosylation and the formation of reactive oxygen species (ROS) in the liver [93]. High fructose diet induces steatosis, inflammation and periportal fibrosis [45,94,95]. High fructose diet induces histopathological changes that is associated with dyslipidaemia, insulin resistance, elevated pro-inflammatory cytokines and markers of lipid peroxidation [30] in rats.

In the present study, MCFD induced significant elevation in MDA as indicator of lipid peroxidation which is indicative to high oxidative stress. Oxidative stress plays a major role in the pathogenesis of NAFLD because of lipid peroxidation which is followed by activation of the inflammatory response and of stellate cells, as a result of the increased production of ROS, leading to fibrogenesis. Lipid peroxidation generally leads to the formation of peroxyl radicals, which are the essential species of the peroxidation chain reaction [96].

Table 4
Different biochemical parameters of normal and fatty liver cirrhotic rats treated with (F7) PSO NE at low and high doses (Mean ± SE).

Parameters	Normal control	MCFD control	PSO NE low dose*	PSO NE high dose**
Plasma				
T-Cholesterol (mg/dl)	68.8 ± 1.346 ^{a}	112 ± 1.914 ^{b}	86.8 ± 1.851 ^{c}	78.7 ± 1.943 ^{d}
Triglycerides (mg/dl)	78.06 ± 1.638 ^{a}	162.2 ± 2.650 ^{b}	130.3 ± 3.979 ^{c}	96.7 ± 1.705 ^{d}
HDL-Ch (mg/dl)	33.2 ± 1.045 ^{a}	21.5 ± 0.619 ^{b}	29 ± 0.730 ^{c}	36.2 ± 0.654 ^{d}
LDL-Ch (mg/dl)	20.3 ± 0.715 ^{a}	67.8 ± 1.887 ^{b}	53 ± 2.250 ^{c}	39.7 ± 1.801 ^{d}
T-Ch/HDL-Ch	2.1 ± 0.078 ^{a}	5.2 ± 0.186 ^{b}	2.9 ± 0.057 ^{c}	2.2 ± 0.064 ^{a}
MDA (nmol/ml)	6.3 ± 0.214 ^{a}	21.8 ± 0.790 ^{b}	17.8 ± 0.654 ^{c}	12.8 ± 0.703 ^{d}
TNF-α (pg/ml)	16.3 ± 0.651 ^{a}	30.3 ± 1.282 ^{b}	23.3 ± 0.615 ^{c}	18.6 ± 0.735 ^{d}
AST (U/l)	51.7 ± 1.202 ^{a}	88.2 ± 1.238 ^{b}	77.7 ± 0.919 ^{c}	67.2 ± 1.939 ^{d}
ALT (U/l)	39.2 ± 1.046 ^{a}	77.5 ± 2.156 ^{b}	65 ± 1.788 ^{c}	45 ± 1.390 ^{d}
ALP (IU/l)	154.7 ± 2.905 ^{a}	201.7 ± 3.333 ^{b}	178.2 ± 3.581 ^{c}	167.3 ± 2.824 ^{c}
Total Bilirubin (mg/dl)	0.327 ± 0.007 ^{a}	0.505 ± 0.009 ^{b}	0.415 ± 0.011 ^{c}	0.372 ± 0.012 ^{d}
Direct Bilirubin (mg/dl)	0.148 ± 0.004 ^{a}	0.255 ± 0.008 ^{b}	0.190 ± 0.008 ^{c}	0.151 ± 0.009 ^{a}
Albumin (g/dl)	3.9 ± 0.108 ^{a}	2.5 ± 0.044 ^{b}	3.1 ± 0.075 ^{c}	3.4 ± 0.058 ^{c}
Liver				
Total fat (mg/g tissue)	25.0 ± 0.894 ^{a}	47.8 ± 1.222 ^{b}	34.8 ± 1.046 ^{c}	27.5 ± 0.764 ^{d}
T-Cholesterol (mg/g tissue)	2.78 ± 0.217 ^{a}	8.70 ± 0.316 ^{b}	7.10 ± 0.206 ^{c}	5.10 ± 0.201 ^{d}
Triglycerides (mg/g tissue)	7.2 ± 0.232 ^{a}	16.7 ± 0.882 ^{b}	11.7 ± 0.667 ^{c}	8.1 ± 0.215 ^{d}

In each row same superscript letters are statistically non-significant different while different superscript letters are statistically significant different at $P < 0.05$.

* Low dose = 50 mg/kg rat body weight.

** High dose = 100 mg/kg rat body weight.

Table 5
Nutritional parameters of different experimental groups.

Groups	Initial body weight (g)	Final body weight (g)	Body weight gain (g)	Total Food intake (g)	Food efficiency ratio	Liver weight/body weight %
Normal control	130.5 ± 8.352	216.2 ± 2.813	85.7 ± 3.791	511.3 ± 6.162	0.168 ± 0.008	3.5 ± 0.173
MCFD control	130.2 ± 2.663	214.5 ± 3.694	84.3 ± 3.158	515.9 ± 5.108	0.163 ± 0.006	3.8 ± 0.116
PSO NE low dose [a]	130.5 ± 2.777	216.2 ± 3.419	85.7 ± 2.939	507.7 ± 2.859	0.168 ± 0.006	3.8 ± 0.124
PSO NE high dose [b]	130.3 ± 2.764	215.3 ± 4.159	85 ± 3.855	509.3 ± 4.087	0.167 ± 0.007	3.5 ± 0.046

Non-significant difference was reported between the different experimental groups.
[a] Low dose = 50 mg/kg rat body weight.
[b] High dose = 100 mg/kg rat body weight.

Oral administration of PSO NEs improved dyslipidemia, oxidative stress and liver dysfunction observed in rats fed on MCFD. PSO NEs also reduced liver total fat, TG and T-Ch which prove that it is able to inhibit the progression to NASH and fibrogenesis. PSO is rich in unsaturated fatty acids mainly linoleic and contain high levels of phytochemicals and phytonutrients represented by total phenolics, beta-carotene, α and δ tocopherol [31,69,97]. These bioactive constituents could be responsible on the bioactivity of PSO. Also the presence of PSO in NE system could be the cause of its efficiency in low doses due to increased bioavailability compared to the previous study [30]. Due to its subcellular and submicrometer size, NE systems may pass fine capillaries even the fenestration present in the epithelial lining in liver resulting in deep penetration into organ tissues. This let efficient delivery of therapeutic agents to target sites in the body [98]. Although PSO NE was not given as a daily dose but only three times a week, it showed promising bioactivity, which could be attributed to its sustained release property. It is reported that small globule size NEs remain for longer periods of time in the circulation after *in vivo* application [38]. In a previous study [30], PSO *per se* showed protective effect towards fatty liver in rats. The rats in that study were weighing 160 g and fed on diet containing 5.5% PSO in addition of a daily oral dose of 200 mg/rat/day.

4. Conclusions

In the present study, pumpkin seed oil was incorporated in nanoemulsion systems, and *in vitro* and *in vivo* evaluated. The optimized formulation; F7, containing PSO (10%), Labrafac™ PG (17%), Tween 80 (31.5%), PEG 400 (31.5%) and water (10%), which possessed the highest *in vitro* release of total phenolic content (100%) after 24 h and optimum physico-chemical parameters, was chosen for the *in vivo* evaluation studies. F7 showed enhanced prevention of progression of fatty liver to steatohepatitis and fibrosis in a steatohepatitis and fibrosis induced rat model. After thirty-five days of oral administration, F7 revealed improvement of plasma lipid profile, malodialdehyde and tumor necrosis factor-α with reduction of liver fat and improvement of hepatic function. The improvement was dose dependent; the high dose (100 mg/kg rat body weight) was more promising compared to 50 mg/kg rat body weight. Hence, the incorporation of PSO in NE systems is a promising technological approach to achieve more beneficial utilization of its bioactive compounds for management of hepatic conditions.

Declaration of interest

The authors report no declarations of interest.

Acknowledgements

The authors would deeply thank the Project's Sector at the National Research Centre, Egypt for funding this work through the research group project fund no. 10090006.

References

[1] M. Yao, D.J. McClements, H. Xiao, Improving oral bioavailability of nutraceuticals by engineered nanoparticle-based delivery systems, Curr. Nutr. Food Sci. 2 (2015) 14–19.
[2] M. Yao, H. Xiao, D.J. McClements, Delivery of lipophilic bioactives: assembly, disassembly, and reassembly of lipid nanoparticles, Annu. Rev. Food Sci. Technol. 5 (2014) 53–81.
[3] C.J. Porter, C.W. Pouton, J.F. Cuine, W.N. Charman, Enhancing intestinal drug solubilisation using lipid-based delivery systems, Adv. Drug Deliv. Rev. 60 (2008) 673–691.
[4] P. Dwivedi, R. Khatik, P. Chaturvedi, K. Khandelwal, I. Taneja, K.S. Raju, H. Dwivedi, S.K. Singh, P.K. Gupta, P. Shukla, P. Tripathi, S. Singh, R. Tripathi, Wahajuddin, S.K. Paliwal, A.K. Dwivedi, P.R. Mishra, Arteether nanoemulsion for enhanced efficacy against *Plasmodium yoelii* nigeriensis malaria: an approach by enhanced bioavailability, Colloids Surf. A Physicochem. Eng. Asp. 126 (2015) 467–475.
[5] K.R. Jadhav, I.M. Shaikh, K.W. Ambade, V.J. Kadam, Applications of microemulsion based drug delivery system, Curr. Drug Deliv. 3 (2006) 267–273.
[6] P.K. Ghosh, R.S. Murthy, Microemulsions: a potential drug delivery system, Curr. Drug Deliv. 3 (2006) 167–180.
[7] G. Mustafa, Z.I. Khan, T. Bansal, S. Talegaonkar, Preparation and characterization of oil in water nano-reservoir systems for improved oral delivery of atorvastatin, Curr. Nanosci. 5 (2009) 428–440.
[8] M. Sivakumar, S.Y. Tang, K.W. Tan, Cavitation technology - a greener processing technique for the generation of pharmaceutical nanoemulsions, Ultrason. Sonochem. 21 (2014) 2069–2083.
[9] K. Frede, A. Henze, M. Khalil, S. Baldermann, F.J. Schweigert, H. Rawel, Stability and cellular uptake of lutein-loaded emulsions, J. Funct. Foods 8 (2014) 118–127.
[10] K. Ahmed, Y. Li, D.J. McClements, H. Xiao, Nanoemulsion- and emulsion-based delivery systems for curcumin: encapsulation and release properties, Food Chem. 132 (2012) 799–807.
[11] J. Zheng, Y. Li, M. Song, X. Fang, Y. Cao, D.J. McClements, H. Xiao, Improving intracellular uptake of 5-demethyltangeretin by food grade nanoemulsions, Food Res. Int. 62 (2014) 98–103.
[12] A. Koteish, A. Mae Diehl, Animal models of steatohepatitis, Best Pract. Res. Clin. Gastroenterol. 16 (2002) 679–690.
[13] K. Mehta, D.H. Van Thiel, N. Shah, S. Mobarhan, Nonalcoholic fatty liver disease: pathogenesis and the role of antioxidants, Nutr. Rev. 60 (2002) 289–293.
[14] S.Y. Al-Okbi, D.A. Mohamed, T.E. Hamed, A.E. Edris, Potential protective effect of *Nigella sativa* crude oils towards fatty liver in rats, Eur. J. Lipid Sci. Technol. 115 (2013) 774–782.
[15] Y. Qian, J.-G. Fan, Obesity, fatty liver and liver cancer, Hepatobiliary Pancreat. Dis. Int. 4 (2005) 173–177.
[16] N. Assy, K. Kaita, D. Mymin, C. Levy, B. Rosser, G. Minuk, Fatty infiltration of liver in hyperlipidemic patients, Dig. Dis. Sci. 45 (2000) 1929–1934.
[17] D.A. Sass, P. Chang, K.B. Chopra, Nonalcoholic fatty liver disease: a clinical review, Dig. Dis. Sci. 50 (2005) 171–180.
[18] E. Bugianesi, N. Leone, E. Vanni, G. Marchesini, F. Brunello, P. Carucci, A. Musso, P. De Paolis, L. Capussotti, M. Salizzoni, Expanding the natural history of nonalcoholic steatohepatitis: from cryptogenic cirrhosis to hepatocellular carcinoma, Gastroenterology 123 (2002) 134–140.
[19] G. Marchesini, M. Brizi, G. Bianchi, S. Tomassetti, M. Zoli, N. Melchionda, Metformin in non-alcoholic steatohepatitis, Lancet 358 (2001) 893–894.
[20] M. Egan, S. Prasad, PURLs: statins for patients with nonalcoholic fatty liver? J. Fam. Pract. 60 (2011) 536–538.
[21] J. Laurin, K.D. Lindor, J.S. Crippin, A. Gossard, G.J. Gores, J. Ludwig, J. Rakela, D.B. McGill, Ursodeoxycholic acid or clofibrate in the treatment of non-alcohol-induced steatohepatitis: a pilot study, Hepatology 23 (1996) 1464–1467.
[22] F. Caili, S. Huan, L. Quanhong, A review on pharmacological activities and utilization technologies of pumpkin, Plant Foods Hum. Nutr. 61 (2006) 70–77.
[23] A.G. Ardabili, R. Farhoosh, M.H.H. Khodaparast, Chemical composition and physicochemical properties of pumpkin seeds (*Cucurbita pepo subsp. pepo* Var. Styriaka) grown in Iran, J. Agric. Sci. Technol. 13 (2011) 1053–1063.
[24] H.S. Paris, Historical records, origins, and development of the edible cultivar groups of *Cucurbita pepo* (Cucurbitaceae), Econ. Bot. 43 (1989) 423–443.
[25] V.V. Markovic, L.V. Bastic, Characteristics of pumpkin seed oil, J. Am. Oil Chem. Soc. 53 (1976) 42–44.
[26] S. Harvath, Z. Bedo, Another possibility in treatment of hyperlipidemia with peponen of natural active substance, Fortschr. Med. 89 (1988) 7–8.
[27] G. Schiebel-Schlosser, M. Friederich, Phytotherapy of BPH with pumpkin seeds–a multicenter clinical trial, Z. Phys. 19 (1998) 71–76.

[28] H.A. Zuhair, A.A. Abd El-Fattah, M.I. El-Sayed, Pumpkin-seed oil modulates the effect of felodipine and captopril in spontaneously hypertensive rats, Pharmacol. Res. 41 (2000) 555–563.
[29] K. Dreikorn, The role of phytotherapy in treating lower urinary tract symptoms and benign prostatic hyperplasia, World J. Urol. 19 (2002) 426–435.
[30] S.Y. Al-Okbi, D.A. Mohamed, T.E. Hamed, R.S. Esmail, Rice bran oil and pumpkin seed oil alleviate oxidative injury and fatty liver in rats fed high fructose diet, Pol. J. Food and Nutr. Sci. 64 (2014) 127–133.
[31] S.Y. Al-Okbi, D.A. Mohamed, E. Kandil, E. Ahmed, S. Mohammed, Functional ingredients and cardiovascular protective effect of pumpkin seed oils, Grasas Aceites 65 (2014) 1–10.
[32] S.Y. Al-Okbi, D.A. Mohamed, E. Kandil, E.K. Ahmed, S.E. Mohammed, Antioxidant and anti-cancer effect of egyptian and european pumpkin seed oil, Res. J. Pharm., Biol. Chem. Sci. 7 (2016) 574–580.
[33] D.M. Mostafa, S.H. Abd El-Alim, M.H. Asfour, S.Y. Al-Okbi, D.A. Mohamed, G. Awad, Transdermal nanoemulsions of *Foeniculum vulgare* Mill. essential oil: Preparation, characterization and evaluation of antidiabetic potential, J. Drug Deliv. Sci. Technol. 29 (2015) 99–106.
[34] S.A. Fouad, E.B. Basalious, M.A. El-Nabarawi, S.A. Tayel, Microemulsion and poloxamer microemulsion-based gel for sustained transdermal delivery of diclofenac epolamine using in-skin drug depot: in vitro/in vivo evaluation, Int. J. Pharm. 453 (2013) 569–578.
[35] S. Akhter, G.K. Jain, F.J. Ahmad, R.K. Khar, N. Jain, Z.I. Khan, S. Talegaonkar, Investigation of nanoemulsion system for transdermal delivery of domperidone: *Ex-vivo* and *in vivo* studies, Curr. Nanosci. 4 (2008) 381–390.
[36] D.M. Mostafa, A.A. Kassem, M.H. Asfour, S.Y. Al Okbi, D.A. Mohamed, T.E. Hamed, Transdermal cumin essential oil nanoemulsions with potent antioxidant and hepatoprotective activities: in-vitro and in-vivo evaluation, J. Mol. Liq. 212 (2015) 6–15.
[37] V. Bali, M. Ali, J. Ali, Nanocarrier for the enhanced bioavailability of a cardiovascular agent: in vitro, pharmacodynamic, pharmacokinetic and stability assessment, Int. J. Pharm. 403 (2011) 46–56.
[38] V. Bali, M. Ali, J. Ali, Study of surfactant combinations and development of a novel nanoemulsion for minimising variations in bioavailability of ezetimibe, Colloids Surf. A Physicochem. Eng. Asp. 76 (2010) 410–420.
[39] V.L. Singleton, J.A. Rossi Jr., Colorimetry of total phenolics with phosphomolybdic-phosphotungstic acid reagents, Am. J. Enol. Vitic. 16 (1965) 144–158.
[40] K. Jain, R.S. Kumar, S. Sood, K. Gowthamarajan, Enhanced oral bioavailability of atorvastatin via oil-in-water nanoemulsion using aqueous titration method, J.Pharm. Sci. Res. 5 (2013) 18–25.
[41] S.K. Mehta, G. Kaur, K.K. Bhasin, Incorporation of Antitubercular drug isoniazid in pharmaceutically accepted microemulsion: effect on microstructure and physical parameters, Pharm. Res. 25 (2008) 227–236.
[42] D.M. Mostafa, N.M. Ammar, M. Basha, R.A. Hussein, S. El Awdan, G. Awad, Transdermal microemulsions of Boswellia carterii bird: formulation, characterization and in vivo evaluation of anti-inflammatory activity, Drug Deliv. 22 (2015) 748–756.
[43] G. Briggs, M. Williams, New mineral mixture for experimental rat diets and evaluation of other mineral mixtures, Federation Proceedings, Federation Amer, Soc. Exp. Biol. 22 (2) (1963) 601–608 9650 Rockville Pike, Bethesda, MD 20814-3998.
[44] S.R. Morcos, The effect of the protein value of the diet on the neurological manifestations produced in rats by β, β-iminodipropionitrile, Br. J. Nutr. 21 (1967) 269–274.
[45] T. Kawasaki, K. Igarashi, T. Koeda, K. Sugimoto, K. Nakagawa, S. Hayashi, R. Yamaji, H. Inui, T. Fukusato, T. Yamanouchi, Rats fed fructose-enriched diets have characteristics of nonalcoholic hepatic steatosis, J. Nutr. 139 (2009) 2067–2071.
[46] R. Deminice, G.S.F. de Castro, L.V. Francisco, L.E.C.M. da Silva, J.F.R. Cardoso, F.T.T. Frajacomo, B.G. Teodoro, L. dos Reis Silveira, A.A. Jordao, Creatine supplementation prevents fatty liver in rats fed choline-deficient diet: a burden of one-carbon and fatty acid metabolism, J. Nutr. Biochem. 26 (2015) 391–397.
[47] D. Watson, A simple method for the determination of serum cholesterol, Clin. Chim. Acta 5 (1960) 637–643.
[48] M. Burstein, H.R. Scholnick, R. Morfin, Rapid method for the isolation of lipoproteins from human serum by precipitation with polyanions, J. Lipid Res. 11 (1970) 583–595.
[49] H. Schriewer, U. Kohnert, G. Assmann, Determination of LDL cholesterol and LDL apolipoprotein B following precipitation of VLDL in blood serum with phosphotungstic acid/$MgCl_2$, J. Clin. Chem. Clin. Biochem. 22 (1984) 35–40.
[50] R.E. Megraw, D. Dunn, H. Biggs, Manual and continuous-flow colorimetry of triacylglycerols by a fully enzymic method, Clin. Chem. 25 (1979) 273–278.
[51] S. Kei, Serum lipid peroxide in cerebrovascular disorders determined by a new colorimetric method, Clin. Chim. Acta 90 (1978) 37–43.
[52] J.A. Stepaniak, K.E. Gould, D. Sun, R.H. Swanborg, A comparative study of experimental autoimmune encephalomyelitis in Lewis and DA rats, J. Immunol. 155 (1995) 2762–2769.
[53] S. Reitman, S. Frankel, Colorimetric methods for aspartate and alanine aminotransferase, Am. J. Clin. Pathol. 28 (1957) 55–60.
[54] B.T. Doumas, W.A. Watson, H.G. Biggs, Albumin standards and the measurement of serum albumin with bromcresol green, Clin. Chim. Acta 31 (1971) 87–96.
[55] S.R. Gambino, in: S. Meites (Ed.), Standard Methods of Clinical Chemistry, Academic Press., New York 1965, pp. 55–64.
[56] J.F. Kochmar, D.W. Moss, in: N.W. Tietz (Ed.), Fundamentals of clinical chemistry, W. B. Saunders and Company, Philadephia, PA. 1976, p. 604.
[57] J. Folch, M. Lees, G. Sloane-Stanley, A simple method for the isolation and purification of total lipids from animal tissues, J. Biol. Chem. 226 (1957) 497–509.
[58] E. Cequier-Sánchez, C. Rodriguez, A.G. Ravelo, R. Zárate, Dichloromethane as a solvent for lipid extraction and assessment of lipid classes and fatty acids from samples of different natures, J. Agric. Food Chem. 56 (2008) 4297–4303.
[59] A.R. Patel, P.R. Vavia, Preparation and in vivo evaluation of SMEDDS (self-microemulsifying drug delivery system) containing fenofibrate, AAPS J. 9 (2007) E344–E352.
[60] P.P. Constantinides, Lipid microemulsions for improving drug dissolution and oral absorption: physical and biopharmaceutical aspects, Pharm. Res. 12 (1995) 1561–1572.
[61] S. Shafiq, F. Shakeel, S. Talegaonkar, F.J. Ahmad, R.K. Khar, M. Ali, Development and bioavailability assessment of ramipril nanoemulsion formulation, Eur. J. Pharm. Biopharm. 66 (2007) 227–243.
[62] M.J. Lawrence, G.D. Rees, Microemulsion-based media as novel drug delivery systems, Adv. Drug Deliv. Rev. 45 (2000) 89–121.
[63] A.R. Dixit, S.J. Rajput, S.G. Patel, Preparation and bioavailability assessment of SMEDDS containing valsartan, AAPS PharmSciTech 11 (2010) 314–321.
[64] S.P. Vyas, R.K. Khar, Submicronemulsions, in: S.P. Vyas, R.K. Khar (Eds.), Targeted and Controlled Drug Delivery: Novel Carrier Systems, CBS Publishers, New Delhi 2002, pp. 280–302.
[65] G. Sukanaya, S. Mantry, S. Anjum, Review on nanoemulsions, Int. J. Pharm. Sci. Res. 1 (2013) 192–205.
[66] B. Xia, W. Ha, X. Meng, T. Govender, S. Peng, L. Ding, B. Li, S. Zhang, Preparation and characterization of a poly(ethylene glycol) grafted carboxymethyl konjac glucomannan copolymer, Carbohydr. Polym. 79 (2010) 648–654.
[67] T. Tadros, P. Izquierdo, J. Esquena, C. Solans, Formation and stability of nano-emulsions, Adv. Colloid Interf. Sci. 108–109 (2004) 303–318.
[68] V. Vujasinovic, S. Djilas, E. Dimic, Z. Basic, O. Radocaj, The effect of roasting on the chemical composition and oxidative stability of pumpkin oil, Eur. J. Lipid Sci. Technol. 114 (2012) 568–574.
[69] M. Andjelkovic, J. Van Camp, A. Trawka, R. Verhé, Phenolic compounds and some quality parameters of pumpkin seed oil, Eur. J. Lipid Sci. Technol. 112 (2010) 208–217.
[70] V. Vujasinovic, S. Djilas, E. Dimic, R. Romanic, A. Takaci, Shelf life of cold-pressed pumpkin (*Cucurbita pepo* L.) seed oil obtained with a screw press, J. Am. Oil Chem. Soc. 87 (2010) 1497–1505.
[71] D. Huang, B. Ou, R.L. Prior, The chemistry behind antioxidant capacity assays, J. Agric. Food Chem. 53 (2005) 1841–1856.
[72] P. Górnaś, K. Dwiecki, A. Siger, J. Tomaszewska-Gras, M. Michalak, K. Polewski, Contribution of phenolic acids isolated from green and roasted boiled-type coffee brews to total coffee antioxidant capacity, Eur. Food Res. Technol. 242 (2016) 641–653.
[73] R.M. Hathout, T.J. Woodman, S. Mansour, N.D. Mortada, A.S. Geneidi, R.H. Guy, Microemulsion formulations for the transdermal delivery of testosterone, Eur. J. Pharma. Sci. 40 (2010) 188–196.
[74] S.K. Mehta, G. Kaur, K.K. Bhasin, Analysis of tween based microemulsion in the presence of TB drug rifampicin, Colloids Surf. A Physicochem. Eng. Asp. 60 (2007) 95–104.
[75] S.K. Mehta, K. Bala, Tween-based microemulsions: a percolation view, Fluid Phase Equilib. 172 (2000) 197–209.
[76] G.S. Grest, I. Webman, S.A. Safran, A.L.R. Bug, Dynamic percolation in microemulsions, Phys. Rev. A 33 (1986) 2842–2845.
[77] K.E. Bennett, J.C. Hatfield, H.T. Davis, C.W. Macosko, L.E. Scriven, Viscosity and conductivity of microemulsions, in: I.D. Robb (Ed.), Microemulsions, Springer US, Boston, MA 1982, pp. 65–84.
[78] L. Djordjevic, M. Primorac, M. Stupar, D. Krajisnik, Characterization of caprylocaproyl macrogolglycerides based microemulsion drug delivery vehicles for an amphiphilic drug, Int. J. Pharm. 271 (2004) 11–19.
[79] C. Mo, X. Li, Microstructure and structural transition in coconut oil microemulsion using semidifferential electroanalysis, J. Colloid Interface Sci. 312 (2007) 355–362.
[80] A.T. Florence, D. Attwood, Emulsions, suspensions and other dispersions, in: A.T. Florence, D. Attwood (Eds.), Physicochemical Principles of Pharmacy, Macmillan Press Ltd, London 1998, pp. 252–307.
[81] F. Podlogar, M. Gašperlin, M. Tomšič, A. Jamnik, M.B. Rogač, Structural characterisation of water–tween 40®/Imwitor 308®–isopropyl myristate microemulsions using different experimental methods, Int. J. Pharm. 276 (2004) 115–128.
[82] C. Qian, D.J. McClements, Formation of nanoemulsions stabilized by model food-grade emulsifiers using high-pressure homogenization: factors affecting particle size, Food Hydrocoll. 25 (2011) 1000–1008.
[83] V. Ghosh, A. Mukherjee, N. Chandrasekaran, Ultrasonic emulsification of food-grade nanoemulsion formulation and evaluation of its bactericidal activity, Ultrason. Sonochem. 20 (2013) 338–344.
[84] A.A. Kassem, A.M. Mohsen, R.S. Ahmed, T.M. Essam, Self-nanoemulsifying drug delivery system (SNEDDS) with enhanced solubilization of nystatin for treatment of oral candidiasis: design, optimization, in vitro and in vivo evaluation, J. Mol. Liq. 218 (2016) 219–232.
[85] R.H. Muller, Zeta Potential and Particle Charge in Laboratory Practice: Introduction to Theory, Practical and Data Interpretation, Wissenschaftliche Verlagsgesellschaft, Stuttgart, 1996 104–108.
[86] T.P. Sari, B. Mann, R. Kumar, R.R.B. Singh, R. Sharma, M. Bhardwaj, S. Athira, Preparation and characterization of nanoemulsion encapsulating curcumin, Food Hydrocoll. 43 (2015) 540–546.
[87] V. Klang, C. Valenta, Lecithin-based nanoemulsions, J. Drug Deliv. Sci. Tech. 21 (2011) 55–76.
[88] G. Chhabra, K. Chuttani, A.K. Mishra, K. Pathak, Design and development of nanoemulsion drug delivery system of amlodipine besilate for improvement of oral bioavailability, Drug Dev. Ind. Pharm. 37 (2011) 907–916.
[89] A.K. Ghoshal, New insight into the biochemical pathology of liver in choline deficiency, Crit. Rev. Biochem. Mol. Biol. 30 (1995) 263–273.
[90] R. Vetelainen, A. van Vliet, T.M. van Gulik, Essential pathogenic and metabolic differences in steatosis induced by choline or methione-choline deficient diets in a rat model, J. Gastroenterol. Hepatol. 22 (2007) 1526–1533.

[91] H. Al-Humadi, S. Theocharis, I. Dontas, V. Stolakis, A. Zarros, A. Kyriakaki, R. Al-Saigh, C. Liapi, Hepatic injury due to combined choline-deprivation and thioacetamide administration: an experimental approach to liver diseases, Dig. Dis. Sci. 57 (2012) 3168–3177.
[92] V. Tahan, F. Eren, E. Avsar, D. Yavuz, M. Yuksel, E. Emekli, N. Imeryuz, C. Celikel, H. Uzun, G. Haklar, N. Tozun, Rosiglitazone attenuates liver inflammation in a rat model of nonalcoholic steatohepatitis, Dig. Dis. Sci. 52 (2007) 3465–3472.
[93] J.S. Lim, M. Mietus-Snyder, A. Valente, J.M. Schwarz, R.H. Lustig, The role of fructose in the pathogenesis of NAFLD and the metabolic syndrome, Nat. Rev. Gastroenterol. Hepatol. 7 (2010) 251–264.
[94] F. Armutcu, O. Coskun, A. Gurel, M. Kanter, M. Can, F. Ucar, M. Unalacak, Thymosin alpha 1 attenuates lipid peroxidation and improves fructose-induced steatohepatitis in rats, Clin. Biochem. 38 (2005) 540–547.
[95] Y.F. Tian, C.T. He, Y.T. Chen, P.S. Hsieh, Lipoic acid suppresses portal endotoxemia-induced steatohepatitis and pancreatic inflammation in rats, World J. Gastroenterol. 19 (2013) 2761–2771.
[96] S. Yang, H. Zhu, Y. Li, H. Lin, K. Gabrielson, M.A. Trush, A.M. Diehl, Mitochondrial adaptations to obesity-related oxidant stress, Arch. Biochem. Biophys. 378 (2000) 259–268.
[97] L. Rezig, M. Chouaibi, K. Msaada, S. Hamdi, Chemical composition and profile characterisation of pumpkin (*Cucurbita maxima*) seed oil, Ind. Crop. Prod. 37 (2012) 82–87.
[98] S. Tamilvanan, Formulation of multifunctional oil-in-water nanosized emulsions for active and passive targeting of drugs to otherwise inaccessible internal organs of the human body, Int. J. Pharm. 381 (2009) 62–76.